Physica A 492 (2018) 39–49

Contents lists available at ScienceDirect

Physica A

journal homepage: www.elsevier.com/locate/physa

Persistence of discrimination: Revisiting Axtell, Epstein and Young

Gérard Weisbuch *

Ecole normale superieure, 24, rue Lhomond, Paris, France
Laboratoire de physique statistique, Département de physique de l'ENS, École normale supérieure, PSL Research University, Université Paris Diderot, Sorbonne Paris Cité, Sorbonne Universités, UPMC Univ. Paris 06, CNRS, 75005 Paris, France

ARTICLE INFO

Article history:
Received 7 June 2017
Available online 18 October 2017

Keywords:
Socio-physics
Social cognition
Discrimination
Dynamics
Attraction basins

ABSTRACT

We reformulate an earlier model of the "Emergence of classes..." proposed by Axtell et al. (2001) using more elaborate cognitive processes allowing a statistical physics approach. The thorough analysis of the phase space and of the basins of attraction leads to a reconsideration of the previous social interpretations: our model predicts the reinforcement of discrimination biases and their long term stability rather than the emergence of classes.

1. Introduction

During the 90s social scientists introduced several thought provocative models of social phenomena, most often using numerical simulations (multi-agent simulations). These models have later been extended by methods and concepts derived from statistical physics such as Master Equations and Mean Field Approximation. A few examples include voters models and imitation processes [1] and the review of Castellano et al. [2] , El Farol and the minority game [3] and [4], diffusion of cultures [5,6]. Revisiting these models provided deeper insight, more precise results and even sometimes corrections.

The questions of the emergence and persistence of classes and discrimination received a lot of attention from social scientists, ethnographers and economists, see e.g. [7] and references within. A very inspiring model entitled "Emergence of Classes in a Multi-Agent Bargaining Model" was proposed by Axtell et al. [8]. We here propose to revisit their approach using a more elaborate model of agent cognition and to compare a mean field approach to our agent based simulation results.

2. The models

2.1. The original model of Axtell, Epstein and Young

Let us briefly recall the original hypotheses and the main results of Axtell et al. [8].

- Framework: pairs of agents play a bargaining game introduced by Nas, Jr. [9] and Young [10]. During sessions of the game, each agent can, independently of his opponent, request one among three demands: L(ow) demand 30 perc. of a pie, M(edium) 50 perc. and H(igh) 70 perc. As a result, the two agents get at the end of the session what they demanded when the sum of both demands is less than the 100 perc. total; otherwise they do not get anything. The

* Correspondence to: Laboratoire de Physique Statistique ENS, 24 rue Lhomond 75005, Paris, France.
E-mail address: weisbuch@lps.ens.fr.

https://doi.org/10.1016/j.physa.2017.09.053
0378-4371/

Table 1
Payoff matrix of the Nash demand game. The first column represents the move of the first player L, M or H. The first row represents the move of her opponent. The figures in the matrix represent the payoff obtained by the first player.

	L	M	H
L	0.3	0.3	0.3
M	0.5	0.5	0
H	0.7	0	0

corresponding payoff matrix is written Table 1. At each step a random pair of agents is selected to play the bargaining game. The iterated game is played for a large number of sessions, much larger that the total number of agents which could then learn from their experience how to improve their performance.
- Learning and memory: Agents keep records of the previous demands of their opponents, e.g. for 10 previous moves.
- Choosing the next move: at each time step, pairs of agent are randomly selected to play the bargaining game. They most often choose the move that optimises their expected payoff using the memory of previous encounters as a surrogate for the actual probability distribution of their opponent's next moves. With a small probability ϵ, e.g. 0.1, they choose randomly among L, M, H.

The main results obtained by Axtell et al. [8] from numerical simulations are:

- They observe different transient configurations which they interpret as "norms", e.g. the equity norm is observed when all agents play M. Because of the constant probability of random noise, the system never stabilises on an attractor, even in the sense of Statistical Physics. The duration of the transients increases exponentially with the memory size and $1/\epsilon$.
- Their most fascinating result is obtained when agents are divided into two populations with arbitrary tags say e.g. one red and one blue. When agents take into account tags for playing and memorising games (in other words when agents play separately two games, one intra-game against agents with the same tag and another inter-game against agents with a different tag) one observes configurations in the inter-game such that one population always play H while the other population plays L; they interpret such inequity norm as the emergence of classes, the H playing population being the upper class.

Equivalent results are obtained when agents are connected via a social network as observed by Poza et al. [11] on a square lattice as opposed to the full connection structure used by Axtell et al. [8]. For some instances, domains with different norms occupy different parts of the lattice. Otherwise, one single domain of agents playing the same norm covers the entire lattice, depending upon the initial conditions.

From now on, we follow a plan starting with the exposition of our own model (Section 2.2). The use of a mean field approximation allows to simply describe the attractors of the dynamics and the different dynamical regimes (Section 3). These results are then compared with those obtained by direct agent based simulations (Section 4), including a thorough survey of the attraction basins. We further proceed with the analysis of the two tagged populations version (Section 5). The discussion compares our results to those of previous models and to magnetic systems. A short conclusion stresses the difference in interpretation of the models in terms of social phenomena (Section 6).

2.2. The moving average and Boltzmann choice cognitive model

We start from the same bargaining game as [8] with a payoff matrix written in Table 1, but using different coding of past experience (moving average of past profits) and choice function (Boltzmann function).

The present model is derived from standard models of reinforcement learning in cognitive science, see for instance [12].

Rather than memorising a full sequence of previous games, agents update 3 "preference coefficients" J_j for each possible move j, based on a moving average of the profits they made in the past when playing j. J_1 is the preference coefficient for playing H, J_2 for M and J_3 for L. The updating process following time interval τ after a transaction is:

$$J_j(t+\tau) = (1-\gamma)\cdot J_j(t) + \pi_j(t), \qquad \forall j, \tag{1}$$

The decrease term in $1-\gamma$ corresponds to discounting the importance of past transactions, which makes sense in an environment varying with the choices of the other players. $\pi_j(t)$ is the actual profit made during the chosen transaction j; the 2 other $J_{j'}$ corresponding to the 2 other choices j' are simply decreased.

These preference coefficients are then used to choose the next move in the bargaining game. Agents face an exploitation/exploration dilemma: they can decide to exploit the information they earlier gathered by choosing the move with the highest preference coefficient or check possible evolutions of profits by trying randomly other moves. Rather than using a constant rate of random exploration ϵ as in [8], the probability of choosing demand j is based on the logit function:

$$P_j = \frac{\exp(\beta J_j)}{\sum_j \exp(\beta J_j)}, \qquad \forall j, \tag{2}$$

where β, the discrimination rate, measures the non-linearity of the relationship between the probability P_j and the preference coefficient J_j. Large β values results in always playing the choice j with the largest J_j, small β values to indifference among the three choices. Economists use the name logit for the Boltzmann distribution. We have earlier shown [13] that the Boltzmann distribution can be derived by maximising a linear combination of expected profits and information gained through exploration, see [14] for a thorough discussion.

Comparing our model with the one proposed by Axtell et al. [8]:

- The moving average corresponds to a gradual rather than abrupt decrease of previous memories, it is based on agent's own experience in terms of profit rather than the observation of her opponents' moves and it uses less memory.
- Boltzmann choice has a random character as the constant probability noise introduced in [8], but furthermore the choice depends upon the differences in experienced profits; we might expect agents to be less hesitant when their previous experience resulted in very different preference coefficients.

3. The mean field approximation

3.1. Derivation of the mean field approximation

The difference Eq. (1) can be changed to a differential equation in the limit of a slow dynamics:

$$\frac{dJ_j}{dt} = -\gamma J_j(t) + \pi_j(t) \tag{3}$$

where the time unit is the average time between the agent's bargaining processes. $\pi_j(t)$ is the profit made by the agent if he chose demand j.

The Mean Field approximation consists in replacing $\pi_j(t)$ by its expected value $\langle \pi_j \rangle$, thereby transforming the stochastic differential equation into a deterministic differential equation.

The time evolution of J_{ij} is thus approximated by the following set of equations:

$$\frac{dJ_j}{dt} = -\gamma J_j + \langle \pi_j \rangle \tag{4}$$

where $\langle \pi_j \rangle$ is given by:

$$\langle \pi_j \rangle = \frac{\sum_i \pi_{ij} \exp(\beta J_i)}{\sum_i \exp(\beta J_i)}; \tag{5}$$

j is the agent's move, i are the 3 possible moves of her opponent, and the π_{ij} (0, 0.3, 0.5, 0.7) are the coefficients of the payoff matrix. The mean field approximation neglects fluctuations among agents representations, their J_j. Hence agent j evaluates the probability of her opponent's moves according to her own estimations, using Boltzmann functions of her own J.

Using statistical physics notation Z:

$$Z = \sum_i \exp(\beta J_i) \tag{6}$$

the internal representation of the agent is thus vector (J_1, J_2, J_3) which components obey dynamics:

$$\frac{dJ_1}{dt} = -\gamma J_1 + (exp(\beta J_1) * 0.7 * exp(\beta J_3))/Z/Z \tag{7}$$

$$\frac{dJ_2}{dt} = -\gamma J_2 + (exp(\beta J_2) * 0.5(exp(\beta J_2) + exp(\beta J_3)))/Z/Z \tag{8}$$

$$\frac{dJ_3}{dt} = -\gamma J_3 + exp(\beta J_3) * 0.3/Z \tag{9}$$

Taking the exponentials as new variables simplifies expressions (7)–(9) and allows to deduce scaling properties. Let:

$$x = exp(\beta J_1),\ J_1 = log(x)/\beta \tag{10}$$

$$y = exp(\beta J_2), \quad J_2 = log(y)/\beta \tag{11}$$

$$z = exp(\beta J_3), \quad J_3 = log(z)/\beta \tag{12}$$

The new equations are:

$$\frac{dx}{\beta dt} = x(-\alpha log(x) + 0.7\frac{xz}{s^2}) \tag{13}$$

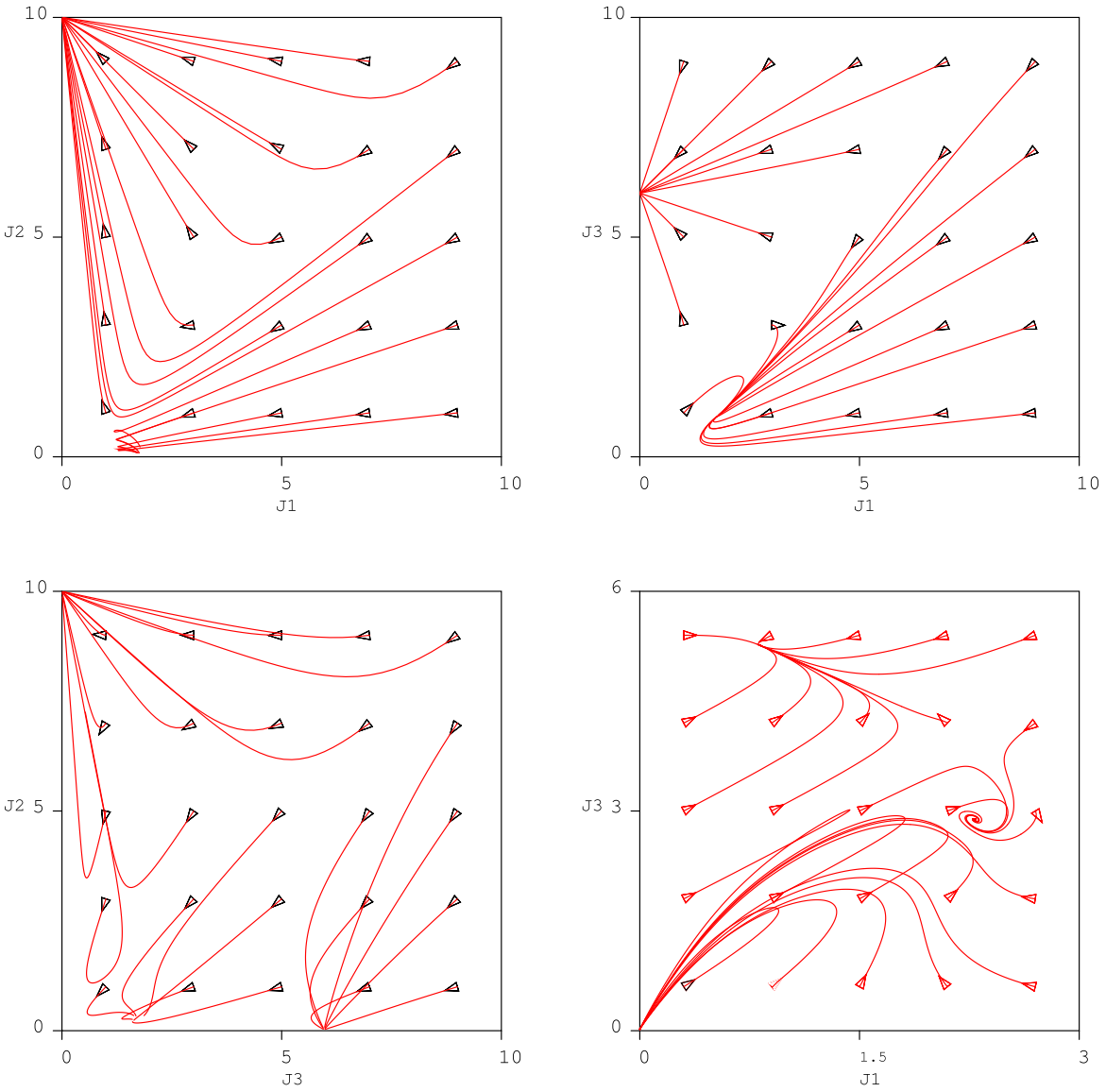

Fig. 1. Grids of trajectories projected on the (J_1, J_2) plan starting from $J_3 = 5$ (above left), on the (J_1, J_3) plan starting from $J_2 = 0.5$ (above right) and on the $(J_3, J2)$ plan starting from $J_1 = 6$ (below left). The black triangles figure the initial conditions of the individual trajectories. $\beta = 2$, $\gamma = 0.05$. The fourth set of projections on the (J_1, J_3) plan starting from $J_2 = 0.5$ (below right) was obtained just above the bifurcation for $\beta = 0.58$. and $\gamma = 0.05$. The L and HL attractors get closer and the basin of attraction of the HL attractor is strongly reduced by the widening of the M attractor. Grind et al. [15] software.

$$\frac{dy}{\beta dt} = y(-\alpha log(y) + 0.5\frac{y(y+z)}{s^2}) \tag{14}$$

$$\frac{dz}{\beta dt} = z(-\alpha log(z) + 0.3\frac{z}{s}) \tag{15}$$

with $s = x + y + z$.

Expressions (13)–(15) show that a single parameter $\alpha = \frac{\gamma}{\beta}$ determines equilibrium conditions, an improvement on [8] who needed two parameters ϵ and memory size. Phase transition diagrams will then be drawn varying β while keeping $\gamma = 0.05$ constant. β plays the role of a kinetic coefficient, increasing the characteristic time towards equilibrium. The magnitude of the J coefficients at equilibrium scales as $1/\gamma$.

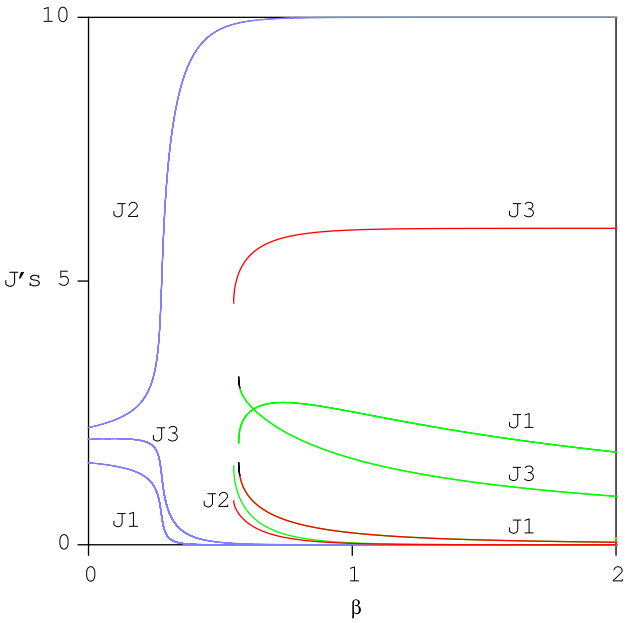

Fig. 2. Bifurcation diagram obtained by integration of the mean field equations. $\gamma = 0.05$. (The continuation algorithm failed to converge to the exact position of the bifurcation around $\beta \approx 0.57$). Attractor M is coloured blue, attractor L is coloured red and attractor HL is coloured green. Grind et al. [15] software. (For interpretation of the references to colour in this figure legend, the reader is referred to the web version of this article.)

3.2. Mean field analysis: Attractors and transitions

The state of the system is described by the set of the preference coefficients J_1, J_2 and J_3 of the agents, i.e. their estimated profit divided by γ for the three possible moves resp. H, M and L. This is an improvement with respect to [8] which space phase dimension was three times the memory size. Our analysis can then proceed using the more powerful methods of dynamical systems and statistical mechanics rather the Markovian formulation proposed in [8].

Trajectories in the **J** phase space are obtained by solving the mean field equations 4–(5) using a Rosenbrock integrator [15]. Grids of trajectories help to figure out attractors and attraction basins. Since we cannot draw sets of 3 trajectories, we display their projections in plans (J_1, J_2) , (J_1, J_3) and (J_3, J_2) for a given choice of $\beta = 2$, $\gamma = 0.05$ in Fig. 1. The trajectories start at regular interval in the projection plan with the same third J coordinate.

Three attractors can be observed: one with large J_2 when move M is the preferred choice by all agents, to be called the M attractor; one with large J_3 when move L is the preferred choice by all agents, to be called the L attractor; and one with lower values of J_1, J_2 and J_3, to be called the HL attractor.

The Mean Field analysis readily tells us that two of the attractors are such that all agents always play the same strategy either M or L.

The dependence of the J's upon the reduced parameter β/γ is displayed on the continuation plot of Fig. 2. We clearly identify the 3 same attractors in the ordered regime above $\beta = 0.57$, and only one attractor left with move M as the preferred choice for lower β values $0.3 < \beta < 0.57$. The bifurcation is observed around $\beta \approx 0.57$. A steep, but not abrupt, transition further occurs when $\beta \approx 0.3$ to a disordered regime such that agents do not display strong preferences for any choice.

4. Agent-based simulations

4.1. Average analysis

Let us now compare the above results with those directly obtained by agent-based simulations. At each time step a pair of agents is randomly chosen. They play the bargaining game choosing their move with a probability given by Eq. (2) using their own specific J_j (not an average J_j as in the mean field approximation), which they update after the session. And so on.

We here report 4 types of results:

- On Fig. 3 the phase transition diagram (to be compared with Fig. 2).
- On Fig. 4 individual trajectories in the J simplex.
- On Fig. 5 the distribution of individual J's on 4 attractors.
- On Fig. 6 a sketch of the attraction basins.

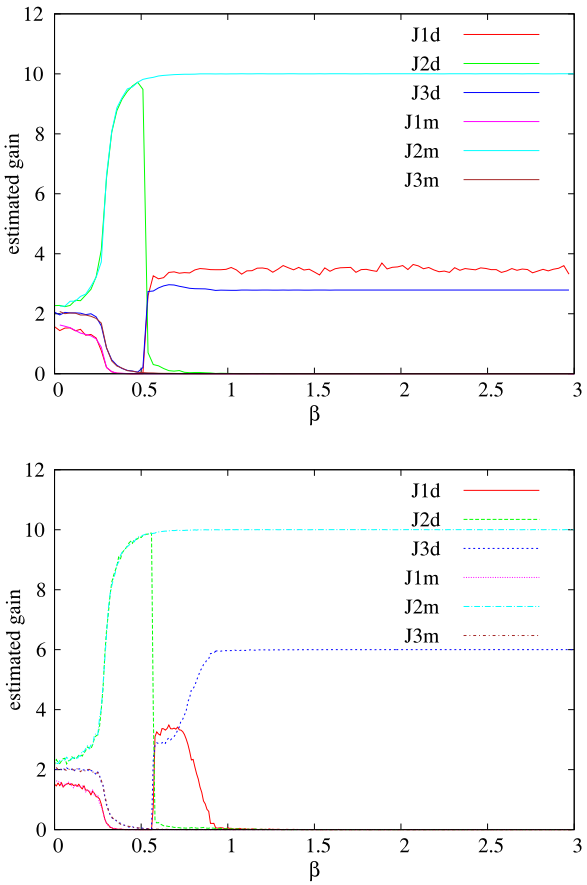

Fig. 3. Bifurcation diagrams obtained by AB simulations. The six lines on each plot are values of the 3 preference coefficients J measured during β decrease between 0 and 2 (J1d e.g.) and then increase (J1m e.g.) from 0 to 2. The decrease is started from the mixed attractor HL on the upper plot, and from the uniform L attractor on the lower plot. Reversibility is only observed in the low β or in the high β region but not across the $\beta = 0.571$ transition.

We first monitor the different J_j averaged over the whole population at equilibrium when β is scanned downward and upward between 0 and 2 (Fig. 3). For the β decreasing branches J_{id}, we start at $\beta = 2$ from initial distributions of J_j close to one of the attractors for each branch and carry on integration until the attractor is reached. The branches are continued when β is lowered, taking as initial conditions the previous values of J_j on the attractor. The equivalent method is applied when β is increased from 0 for the J_{im} branches. For the sake of clarity, attractors HL and attractor L are represented resp. on the upper and lower plots.

Only attractor M can be reached when β is increased from the disordered attractor. When $\beta > 0.571$, the path is reversible, but a hysteresis cycle is observed when β crosses the bifurcation.

In the ordered region, the transition from attractor HL to attractor M is direct. By contrast, one first observes a continuous transition from L to HL around $\beta = 0.75$ above the sharp transition at the bifurcation.

Some attractor levels can be readily obtained from equilibrium conditions of Eqs. 10–(12). When only one move j is chosen by the agents, the fraction involving exponentials equals 1 and the value of J_j is given by :

$$J_j = \frac{\pi_i}{\gamma} \tag{16}$$

in accordance with simulation results: on attractor M J_2 reaches $0.5/0.05 = 10$ and on attractor L J_3 reaches $0.3/0.05 = 6$. In the case of the disordered attractor for low β values, the exponentials are close to one and the J_j are directly computed from Eqs. 10–(12).

Phase diagrams of the mean field approximation and of the agent-based simulations look pretty similar with the same attractors; the main difference is the dependence of **J** upon β for the HL attractor observed in the Mean Field Approximation.

4.2. Individual positions

The previous results concerned global features. Let us now examine individual agent choices. We use a simplex representation as in [8]. At any time step, preference coefficients J of an agent are displayed on the simplex by a point

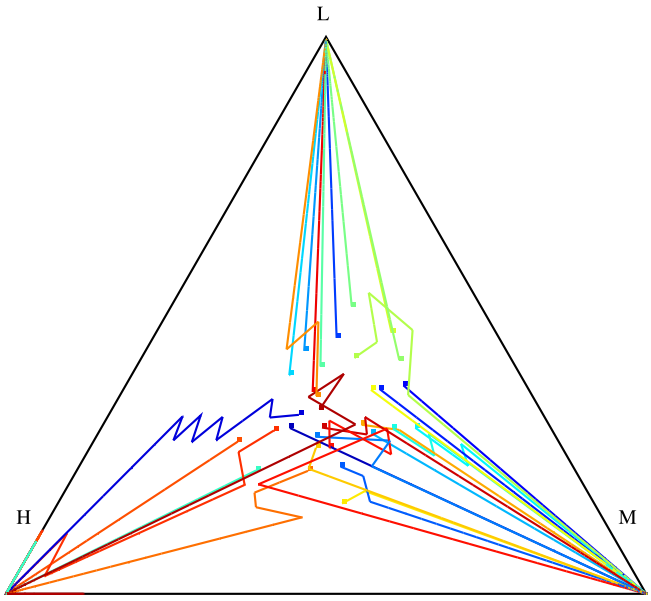

Fig. 4. Individual trajectories across the simplex. Initial positions close to the centre are indicated by little squares. $\beta = 2, \gamma = 0.95$, 10000 integration steps. (For interpretation of the references to colour in this figure legend, the reader is referred to the web version of this article.)

which position corresponds to the centre of gravity of masses proportional to J1, J2, J3 placed at vertices H, M, L. For instance an agent positioned close to the centre of the simplex is indifferent to choice H, M or L, while any agent close to one of the vertices has strong preferences and mostly plays according to that vertex.

Fig. 4 represents a typical set of 30 agents trajectories in the simplex for $\beta = 2$ and $\gamma = 0.05$ during 10000 integration steps (each agent has been sampled 666 times on average). We started from a uniform distribution of initial J's of width 2 centred around (2.0, 2.0, 2.0). Their positions are indicated by a small square. Trajectories are distinctively coloured. After a few initial wanderings, they diverge in the direction of the closest vertex. They remain fixed in the case of L and M vertices. Some might fluctuate around vertex H because of possible encounters with high demanding opponents which result in the decrease of J_3.

Each of the 16 simplices on Fig. 5 is a snapshot of agents' Js after a given integration time for a given value of β and for $\gamma = 0.05$.

Each red point represents the set of preference coefficients of a single agent. Each line of vertices displays the evolution of agents preferences at increasing iteration times towards one of the 4 asymptotic configurations for a given value of β.

The initial conditions where chosen to favour the attractor to be displayed. We used uniform distributions of width 1.0 around (0.9, 0.9, 0.9) for the disordered attractor, D, around (1.0, 0.6, 1.0) for the M attractor, around (1.0, 0.6, 3.0) for the HL attractor and around (0.6, 0.6, 6.5) for the L attractor.

In agreement with previous observations, we see on the first line of Fig. 5 that for low β values the agents positions remain dispersed inside the simplex even for long iteration times, which corresponds to a disordered phase.

By contrast when β is increased, agents in the ordered phase gather towards one or two vertices, even after much smaller iteration times. We have chosen intermediate values of β to avoid the accumulation of representative points on simplex vertices which would be observed at larger β values, e.g. $\beta = 2$.

A physical interpretation of the above results would be a comparison with a condensed phase with thermal excitations above the ground state. When β further increases, an equivalent of temperature decrease in physical systems, agents preferences condense exactly on the vertices (see further Fig. 6), a property which helps us to check the basins of attraction.

4.3. Basins of attraction

The next question concerns the extension of the basins of attraction of the different attractors. In fact, a systematic search for $\beta = 2, \gamma = 0.05$ displays many more attractors than expected from our preliminary scans.

Figuring basins of attraction in a 3D phase space is not obvious and we once again use a vertex representation. The data are obtained by a triple scan of initial conditions. Each initial condition is a uniform distribution of J's values of width 1.0 around a given centre. For instance, an initial distribution centred on the centre of gravity of the simplex is randomly drawn in the cube: $2.7 < J_1 < 3.7$, $2.7 < J_2 < 3.7$, $2.7 < J_3 < 3.7$. The upper circle of Fig. 6 corresponds to the initial distribution: $0.3 < J_1 < 1.3$, $0.3 < J_2 < 1.3$, $2.7 < J_3 < 3.7$ etc.

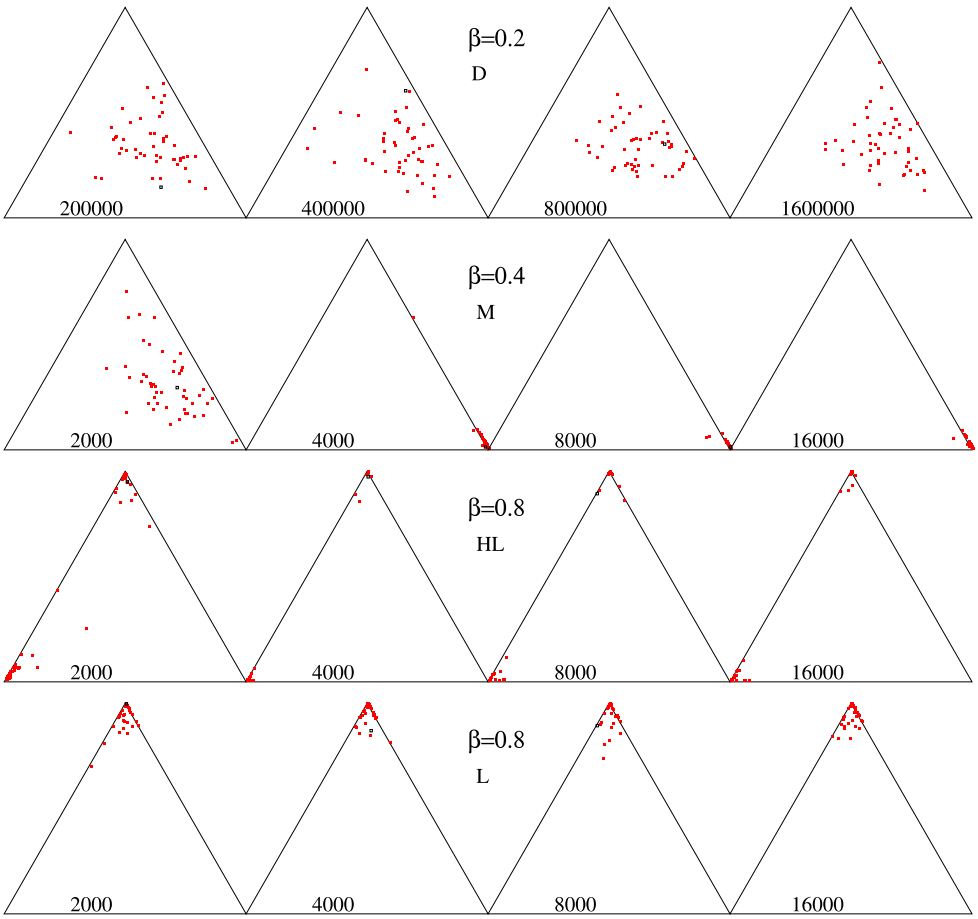

Fig. 5. Evolution of agents positions for different values of β. $\gamma = 0.05$. Each 4 simplex line represents the position of agents J's after different iteration times written at the bottom of the simplex. β values are 0.2, 0.4 and twice 0.8 for the different lines. Initial conditions are given in the text.

Fig. 6 describes data gathered by 3 nested loops across initial J_1, J_2, J_3, where distribution centres are varied from 0.4 to 6.4 by a factor 2. The positions of the centres of the circles in the simplex codes the initial distribution centres. We used the condensation of agents preferences on the 3 vertices to display final distributions by pie charts. Red sectors represent the percentage of agents with choice H, blue sectors represent the percentage of agents with choice M, green sectors represent the percentage of agents with choice L. Rare and narrow white sectors represent the percentage of agents inside the simplex. We checked that they are located in the immediate neighbourhood of vertices.

Several important conclusions about ordered phases for large β can be drawn:

- Mixed strategies inside the vertex are unstable.
- The attractors are distributions of agents on the vertices or very close. Agents have strong opinions about the value of their choice and do not change them frequently.
- J space is paved with basins of attraction surrounding the attractors. The dynamics collapse choices to the nearest vertex, with the exception of vertex H.
- No distribution consists of only H preferences—which would give no gain to the agents. When the initial conditions are close to vertex H, the attractors can only be mixed distributions, with very few agents playing M.
- Axtell et al. [8] and Poza et al. [11] report the existence of "fractious attractor" such that agents oscillate between choices H and L for long transient. We never observed such "fractious attractor", even after a specific search, and we suspect that they were due to their choice of a constant noise term.

5. Tagged populations

The most striking result in [8] is the existence of an inequity norm sustainable among two *a priori* equivalent tagged groups. Their inequity norm corresponds in our settings to an attractor such that all members of one population with tag T1 play H against any member of the other tagged population (T2) who always plays L against them.

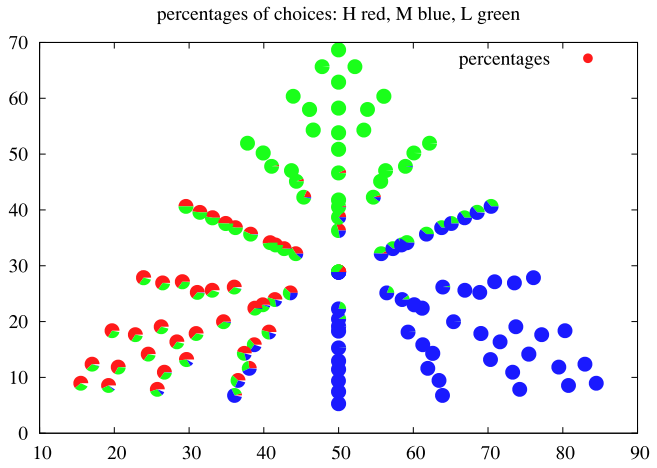

Fig. 6. Simplex representation of the basin of attractions. The position of the circles in the simplex codes the initial conditions. Each circle codes the percentage of agents who reached the 3 vertices. Red sectors represent the percentage of agents with choice H, blue sectors represent the percentage of agents with choice M, green sectors represent the percentage of agents with choice L. Rare and narrow white sectors represent the percentage of agents inside the simplex. $\beta = 2.0$, $\gamma = 0.05$, 100 agents, 100000 iteration steps. (For interpretation of the references to colour in this figure legend, the reader is referred to the web version of this article.)

To investigate the basins of attractions for the two tagged populations we proceed with the same scan of initial conditions of population with tag T2 as above, but maintain the same initial conditions for population with tag T1 around the centre of the simplex:

$2.5 < J_1 < 3.5\,,\ 2.5 < J_2 < 3.5\,,\ 2.5 < J_3 < 3.2.$

Fig. 7 displays the attractors of the inter-population dynamics, the simplex T1 above simplex T2 with the same conventions as in Fig. 5, except that the positions on both simplices correspond to the scan of initial conditions of population T2. The colour codes are the same as for Fig. 6 and reflects the attractors of each population.

The pie charts close to the left vertices of the simplices e.g. are coloured green for T1 and red for T2; the attractors of the dynamics are then L for T1 and H for T2. The pie charts close to the top vertices correspond to a stable mixture of the 3 possible moves H, M, L for T1 and to pure L for T2 The pie charts close to the right vertices correspond to a stable mixture of 2 possible moves M, L for T1 and to pure M for T2.

Not surprisingly, the attractors reflect the initial conditions of population T2 since the initial conditions of T1 were kind of neutral.

The main difference with the no-tag simulation is the appearance of a pure strategy attractor such that all agents with tag T2 play H against agents with tag T1 who play L. This asymmetrical attractor parallel the findings of Axtell et al. [8] who refer to a "discriminatory norm". But our analysis characterises an attractor reached from initial conditions that were already biased towards inequity with larger values of J_1. And this condition is an attractor of the dynamics, not a transient.

6. Discussion and conclusions

The reformulation of the iterated bargaining game of Axtell et al. [8] using more elaborate cognitive processes such as taking moving averages of past gains and choosing next moves according to Boltzmann probabilities allows a more precise description of the dynamics in terms of attractors, regime transitions and basins of attraction. The number of parameters was reduced from two to one. Several transitions are observed between a disordered state and several stable ordered configurations when β increases. Because we use Boltzmann choice function, agents end-up using mostly pure strategies for larger values of β. We never observed any "fractious state" such that agents remain in the interior of the simplex changing randomly their choice between H and L as reported in [8,11]. Our guess is that such behaviour is due to their hypothesis of a random choice with a constant non-zero probability.

As discussed earlier in Sections 5 and 4.3, **J** space is paved with basins of attraction surrounding the attractors and dynamics collapse preference coefficients to the nearest vertex. Unbiased random initial conditions never generate H/L attractors.

Hence our interpretation in terms of social phenomena: game interactions and cognitive processes can increase and stabilise discrimination and inequality among tagged populations, even when tag were *a priori* neutral. On the other hand, inequality attractors never "emerge"[1] spontaneously from random unbiased initial conditions.

[1] [8] specify in a footnote that they "use the term "emergent" ... to mean simply "arising from the local interactions of agents". ". But the word Emergence in the title of their paper evokes the idea of emergence of Classes in a previously egalitarian society.

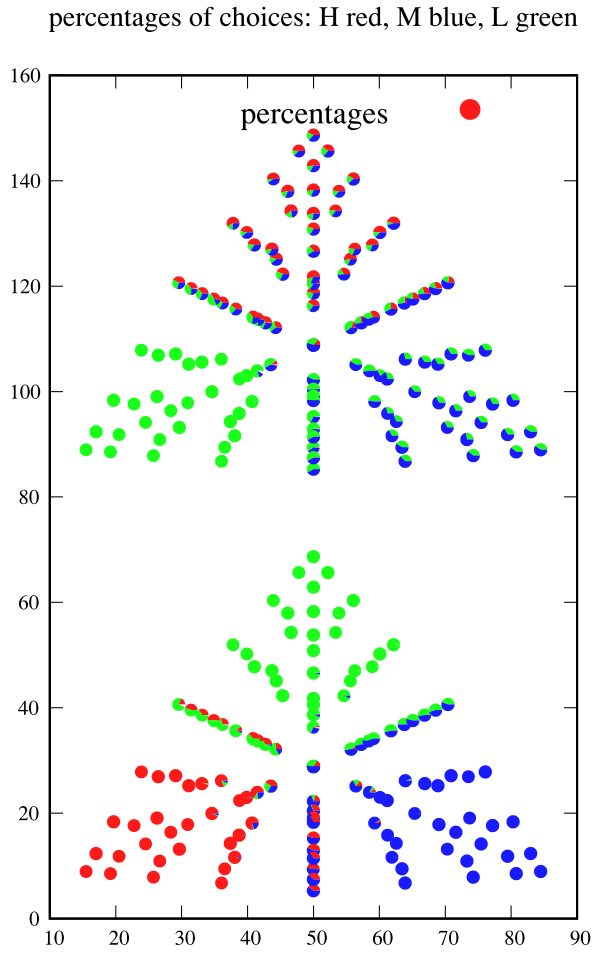

Fig. 7. Simplex representations of the basin of attractions for two tagged populations of 100 agents, one with tag T1 above and one with tag T2 below. As previously, colours code the attractors of the dynamics with the same coding as in Fig. 6. Positions in the simplex code the initial conditions of players with tag T2 *for both groups* while initial conditions of tag T1 players remain identical around the centre of the simplex. $\beta = 2.0$, $\gamma = 0.05$, 100 000 iteration steps per data. (For interpretation of the references to colour in this figure legend, the reader is referred to the web version of this article.)

The changes we introduced in [8] also allow to figure out which properties can be considered as generic, that is to say independent from the details of each model, and which are specific to the exact formulation of the model.

The two versions of the iterated bargaining game, [8] and the present paper, agree that unfair social institutions such as classes and discrimination can result as the downside of a rational cognitive practice, namely memorising or coding previous events to take present decisions. And furthermore, that taking into account *a priori* irrelevant tags can lead to a dissociation of the two tagged populations into an upper and a lower class.

But we differ by our interpretation in terms of social phenomena: game interactions and cognitive processes can increase and stabilise discrimination, but inequality attractors never "emerge" spontaneously from random unbiased initial conditions. History has taught us that wars and invasions often result into discriminations that are maintained long after these events.

Acknowledgements

We thank Sophie Bienenstock, Bernard Derrida, Alan Kirman, Jean-Pierre Nadal and Jean Roux for helpful discussions and David Poza for providing his Netlogo program of the lattice version of Axtell et al. [8] model.

References

[1] A. Nowak, J. Szamrej, B. Latané, From private attitude to public opinion: A dynamic theory of social impact, Psychological Rev. 97 (3) (1990) 362.
[2] C. Castellano, S. Fortunato, V. Loreto, Statistical physics of social dynamics, Rev. Modern Phys. 81 (2) (2009) 591.
[3] W.B. Arthur, Bounded rationality and inductive behavior (the El Farol problem), Am. Econ. Rev. 84 (2) (1994) 406–411.

[4] D. Challet, M. Marsili, Y.-C. Zhang, et al., Minority Games: Interacting Agents in Financial Markets, in: OUP Catalogue, 2013.
[5] R. Axelrod, The dissemination of culture a model with local convergence and global polarization, J. Conflict Resolut. 41 (2) (1997) 203–226.
[6] C. Castellano, M. Marsili, A. Vespignani, Nonequilibrium phase transition in a model for social influence, Phys. Rev. Lett. 85 (16) (2000) 3536.
[7] S. Bowles, S. Naidu, Persistent Institutions. Tech. Rep. Working Paper, Santa Fe Institute, 2006.
[8] R.L. Axtell, J.M. Epstein, H.P. Young, The emergence of classes in a multiagent bargaining model, Soc. Dyn. (2001).
[9] J.F. Nas, Jr., The bargaining problem, Econometrica (1950) 155–162.
[10] H.P. Young, An evolutionary model of bargaining, J. Econom. Theory 59 (1) (1993) 145–168.
[11] D.J. Poza, J.I. Santos, J.M. Galán, A. López-Paredes, Mesoscopic effects in an agent-based bargaining model in regular lattices, PLoS One 6 (3) (2011) e17661.
[12] G. Weisbuch, A. Kirman, D. Herreiner, Market organisation and trading relationships, J. Econ. 110 (463) (2000) 411–436.
[13] J.-P. Nadal, G. Weisbuch, O. Chenevez, A. Kirman, A formal approach to market organization: Choice functions, mean field approximation and maximum entropy principle, in: Advances in Self-Organization and Evolutionary Economics, Economica, London, 1998, pp. 149–159.
[14] J.-P. Bouchaud, Crises and collective socio-economic phenomena: Simple models and challenges, J. Stat. Phys. 151 (3–4) (2013) 567–606.
[15] E. Grind, R.J. de Boer, L. Pagie, GRIND GReat INtegrator Differential Equations, in: Theoretical Biology, Utrecht University, 2017.